Available online at www.sciencedirect.com
ScienceDirect
Journal of Molecular Catalysis B: Enzymatic 54 (2008) 83–89
JOURNAL OF MOLECULAR CATALYSIS B: ENZYMATIC
www.elsevier.com/locate/molcatb

Characterization of lysine-tagged *Bacillus stearothermophilus* leucine aminopeptidase II immobilized onto carboxylated gold nanoparticles

Chien-Li Wu [a], Yi-Pu Chen [a], Jia-Ci Yang [a], Huei-Fen Lo [b,*], Long-Liu Lin [a,**]

[a] *Department of Applied Chemistry, National Chiayi University, 300 University Road, Chiayi 60083, Taiwan*
[b] *Department of Food and Nutrition, Hungkuang University, Taichung 433, Taiwan*

Received 18 July 2007; received in revised form 10 December 2007; accepted 22 December 2007
Available online 4 January 2008

Abstract

Bacillus stearothermophilus leucine aminopeptidase II tagged C-terminally with either tri- or nona-lysine (BsLAPII-$Lys_{3/9}$) was constructed and over-expressed in *Escherichia coli* M15 (pRep4). The recombinant enzymes were purified to homogeneity by nickel-chelate chromatography and their molecular masses were determined to be approximately 45 kDa by SDS/PAGE. Surface modification of colloidal gold with 16-mercaptohexadecanoic acid was employed to generate the carboxylated nanoparticles. BsLAPII-Lys_9 was efficiently immobilized onto the carboxylated gold nanoparticles (AuNP-COOH) and the obtained bioconjugate showed excellent biocatalytic activity in the immobilized form. Additionally, the bioconjugate material exhibited a significant enhancement in temperature stability and could be reused over 5 successive cycles.

Keywords: *Bacillus stearothermophilus*; Leucine aminopeptidase; *Escherichia coli*; Lysine tag; Gold nanoparticles; Immobilization

1. Introduction

There is growing interest in the use of nanoparticles modified with biomolecules for the rational design of nanostructured functional materials [1–5]. Metallic and semiconductor nanoparticles can now be synthesized from a wide range of materials, showing fascinating properties due to their small dimensions [6,7]. Gold nanoparticles (AuNPs) have attracted much more attention in recent years especially because of their biocompatibility to a range of biomolecules such as amino acids [8,9], proteins/enzymes [10–14], and DNA [15,16]. They can provide an environment that is similar to the nature for enzyme immobilization [17]. However, the grafting of proteins onto metal nanoparticels is especially complicated since the conformation of a protein is liable to change through nonspecific interactions, leading to lose its unique biocatalytic activities [18]. Among methods that specifically anchor and separate a concerned protein, recombinant protein synthesis with an affinity ligand at the N- or C-terminal might be a breakthrough to avoid nonspecific interactions. A surface modified by Co^{2+}-nitrilotriacetic acid, for instance, has been used for the specific binding of histidine-tagged proteins [19]. Ethylene glycol monolayer has also been reported to considerably suppress the nonspecific adsorption and the subsequent denaturation of proteins [20,21].

Aminopeptidases are widely distributed exopeptidases that selectively remove the N-terminal amino acid residues from peptides and proteins. They are shown to be essential for protein maturation, degradation of nonhormonal and hormonal peptides, and determination of protein stability [22,23]. With respect to the relative efficiency on which residues are removed, leucine aminopeptidase (LAP) removes most effectively Leu and other hydrophobic residues from peptide substrates [22]. From the view point of commercial applications, LAP is useful for improving the bitter off-taste of protein hydrolysates [24] and for biotransforming L-homophenylalanyl amide to L-homophenylalanine, the versatile intermediate for a class of angiotension I-converting enzyme inhibitors [25]. Earlier, we have cloned and over-expressed the soluble form of *Bacillus stearothermophilus* LAP II (BsLAPII) in recombinant *Escherichia coli* [26]. BsLAPII consists of two identical 44.5-kDa subunits and shows a marked preference for leucine-*p*-nitroanilide (Leu-*p*-NA). The recombinant enzyme is sensitive to oxidative damage by H_2O_2, leading to the disassociation of the

* Corresponding author. Tel.: +886 4 26318652.
** Corresponding author. Fax: +886 5 2717901.
E-mail addresses: hflo@sunrise.hk.edu.tw (H.-F. Lo), llin@mail.ncyu.edu.tw (L.-L. Lin).

1381-1177/$ – see front matter © 2008 Elsevier B.V. All rights reserved.
doi:10.1016/j.molcatb.2007.12.024

dimeric structure [27]. To identify the histidine residues essential for the catalytic activity of BsLAPII, site-directed mutagenesis was performed on the four conserved His residues of the enzyme [28]. Since the Leu substitutions of His-345 and His-378 made the enzyme inactive, we proposed these two residues to be important for the proper function of the enzyme. In this study, we demonstrate the manufacture of a highly water dispersive gold nanoparticles that can efficiently immobilize the lysine-tagged BsLAPII. BsLAPII-Lys_9 binds strongly to the gold nanoparticles and retains a considerable enzymatic activity.

2. Materials and methods

2.1. Materials, bacterial strains, and growth conditions

$HAuCl_4 \cdot 3H_2O$ (99.9%), citric acid (trisodium salt, 99%), and 16-mercaptohexadecanoic acid (MHA, 90%) were obtained from Sigma–Aldrich Fine Chemicals (St. Louis, MO, USA). The oligonucleotides used were synthesized by Mission Biotechnology Inc. (Taipei, Taiwan). Restriction enzymes were purchased from Promega Life Sciences (Madison, WI, USA). Nickel nitrilotriacetate (Ni^{2+}-NTA) resin was acquired from Qiagen Inc. (Valencia, CA, USA). Reagents for polyacrylamide electrophoresis including acrylamide, bisacrylamide, ammonium persulfate, and TEMED were the products of Bio-Rad Laboratories (Hercules, CA, USA). All the solvents otherwise specified were reagent grade, and triply distilled water of resitivity greater than 18.0 MΩ cm was used in making solutions.

E. coli Novablue (Novagen Inc., Madison, WI, USA) was used for the preparation and construction of recombinant plasmids. *E. coli* M15 (pRep4) from Qiagen was used for T5 RNA polymerase-mediated expression of wild-type and Lys-tagged BsLAPIIs. The *E. coli* cells harboring plasmids were grown aerobically at 37 or 28 °C in Luria-Bertani (LB) medium supplemented with 100 μg ampicillin/ml for Novablue strain or 100 μg ampicillin/ml and 25 μg kanamycin/ml for M15 (pRep4) strain.

2.2. Construction, expression and purification of BsLAPII-$Lys_{3/9}$

To construct plasmids encoding BsLAPII fused with Lys tags at the C-terminal end, PCR amplification reactions were performed with 1 U of *Taq* DNA polymerase, 0.25 μM of each synthetic primer, 10 μM of each deoxynucleotide triphosphate, and the buffer recommended by the manufacturer. These amplifications were done in a PerkinElmer thermal cycler (GeneAmp PCR system 2400). The *lap* gene was amplified from pQE-LAPII [26] with the forward primer LAPIIf (5′-GAGGATCCGTTGGGAGAAGGAA-3′), and the reverse primers LAPIIr-Lys_3 (5′-AAGCTTTTACTTCTTCTTCGCCAGTTCGAATGCCCAGTT-3′) and LAPIIr-Lys_9 (5′-AAGCTTTTACTTCTTCTTCTTCTTCTTCTTCTTCGCCAGTTCGAATGCCCAGTT-3′). The PCR amplification was initiated at 94 °C for 3 min followed by 30 cycles of denaturation at 94 °C for 2 min, annealing at 52 °C for 1.5 min, and extension at 74 °C for 2 min, with a final extension at 74 °C for 10 min. The PCR products were analyzed on 1% agarose gel and purified using the DNA extraction kit (Viogene, Sunnyvale, CA, USA). The recovered products were cloned as the *Bam*HI-*Hin*dIII fragments into the corresponding sites of pQE-30 to yield pQE-LAPII-Lys_3 and pQE-LAPII-Lys_9, respectively.

For high-level expression of BsLAPII-Lys_3 and BsLAPII-Lys_9, *E. coli* M15 (pRep4) harboring either pQE-LAPII-Lys_3 or pQE-LAPII-Lys_9 was grown at 37 °C in 100 ml of LB medium supplemented with the above-mentioned antibiotics to an optical density at 600 nm of approximately 1.0. Isopropyl-β-D-thiogalactopyranoside (IPTG) was added to a final concentration of 0.5 mM and the cultivation proceeded at 28 °C for 12 h. The cells were harvested by centrifugation, resuspended in 3 ml of binding buffer (5 mM imidazole, 0.5 M NaCl, and 20 mM Tris–HCl; pH 7.9), and disrupted by sonication. The crude extracts were clarified by centrifugation and the total soluble proteins were mixed with Ni^{2+}-NTA resin pre-equilibrated with the binding buffer. Then, the columns were extensively washed with 20 mM Tris–HCl buffer (pH 7.9) containing 50 mM imadazole and 0.5 M NaCl, until no protein was detected in the eluate by measuring the A_{280}. The His_6-tagged enzymes were eluted from the resin by a buffer containing 0.5 M imidazole, 0.5 M NaCl and 20 mM Tris–HCl (pH 7.9).

2.3. Electrophoresis and determination of protein concentrations

Sodium dodecylsulfate–polyacrylamide gel electrophoresis (SDS/PAGE) with 4% polyacrylamide stacking and 10% polyacrylamide separating gels was performed with the Bio-Rad Mini-Protean III using the Laemmli buffer system [29]. Protein bands were stained with 0.25% Coomassie brilliant blue dissolved in 50% methanol–10% acetic acid, and destined in a 30% methanol–10% acetic acid solution.

Protein concentrations were determined by the Bradford method [30] with the Bio-Rad protein assay reagent, and bovine serum albumin was used as the reference standard.

2.4. Enzyme assay

LAP activity was assayed spectrophotometrically by monitoring the hydrolysis of Leu-*p*-NA [31]. The reaction mixture contained 2.0 mM Leu-*p*-NA, 50 mM Tris–HCl buffer (pH 8.0), 1.0 mM $CoCl_2$, and appropriate amount of the purified enzyme in a final volume of 500 μl. The mixture was incubated at 60 °C for 10 min and the reaction was terminated by the addition of 500 μl of 30% (v/v) acetic acid. The extent of hydrolysis was measured by determining the absorbance at 405 nm and reaction mixtures in the absence of enzyme was used as blanks. One unit of LAP activity is defined as the amount of enzyme that releases 1 μmol of *p*-nitroaniline (*p*-NA) per min at 60 °C.

The K_m and k_{cat} values were estimated by measuring *p*-NA production in 0.5 ml reaction mixtures containing various concentration of the substrate (0.3–2.0 K_m) in 50 mM Tris–HCl buffer, pH 8.0, and a suitable amount of enzyme. Samples were incubated for 10 min at 60 °C. The K_m and k_{cat} values were calculated from the rate *p*-NA production using Michaelis–Menten equation.

2.5. AuNP synthesis

The aqueous AuNP was prepared by following the procedures described in literature [32]: 120 mg of $HAuCl_4$ was initially dissolved in 250 ml of water, and the solution was brought to boiling. A solution of 1% sodium citrate (50 ml) was then added to the $HAuCl_4$ solution under vigorous stirring, and boiling was continued for 60 min. Then, the AuNP solution was cooled down to ambient temperature and the final volume was adjusted to 250 ml with distilled water, which resulted in the AuNP concentration of 18 nM. The resulting deep red solution was monitored by UV–vis spectroscopy on a Shimadzu dual beam spectrometer (Model UV-1601 PC) operated at a resolution of 1 nm and showed the characteristic surface plasmon band at 522 nm.

The morphology and size distribution of the nanoparticles were studied in a Zeiss-EM902 transmission electron microscope using an acceleration voltage of 200 kV. The samples for examination by TEM were prepared by evaporation of a drop of nanoparticle solution on carbon films supported on standard copper grids. Mean particle size and standard deviation were determined from measurement of at least 100 particles.

2.6. MHA modification of AuNP and enzyme immobilization

Since MHA molecules are not soluble in an aqueous solution, ethanol solution containing 5 mM MHA was dropwisely added to the AuNP solution to make a final concentration of 0.5 mM. Subsequently, the AuNP solution was heated up to 90 °C during the addition of MHA without any surfactant, which is often used to avoid particle aggregation. Mild heating was continued for 2 h and the solution was cooled down to ambient temperature. After aging for 24 h at ambient temperature, insoluble precipitate of MHA was removed by extraction with chloroform and again adjusted to the initial volume with distilled water. The FT-IR spectra of free MHA and the adsorbed species on gold nanoparticle surfaces were recorded with a PerkinElmer Spectrum One FT-IR spectrometer. The experiment was carried out at 25 °C, unless otherwise mentioned.

Enzyme immobilization was carried out by soaking the AuNP-COOH with BsLAPII/BsLAP-Lys_3/BsLAP-Lys_9 solution (0.15 mg/ml in 25 mM Tris–HCl buffer, pH 8.0) for 2 h. Adsorbed enzymes on AuNP-COOH were separated from unbound one by centrifugation and re-dispersed in buffer solution for further characterizations.

2.7. pH and temperature effects on immobilized BsLAPII-Lys_9

The pH-dependent variations in catalytic activity of free and biocojugate enzyme were studied at eight different pH values (pH 2, 3 and 4, 20 mM citrate–phosphate buffer; pH 5 and 6, 20 mM Tris–maleate buffer; pH 7, 20 mM potassium phosphate buffer; pH 8 and 9, 20 mM Tris–HCl buffer) by preincubating for 30 min at 4 °C. Thereafter, the residual LAP activity was determined under the standard assay conditions. Reproducibility of the data was tested in three separate measurements carried out under identical conditions.

The temperature stability of free and bioconjugate enzyme was checked by preincubating the samples in 20 mM Tris–HCl buffer (pH 8) at various temperatures (30–80 °C) for 10 min. The residual activity was determined according to the assay method described earlier. Three separate measurements were done to check the reproducibility of the assay.

3. Results and discussion

3.1. Expression and purification of wild-type and poly-lysine-tagged BsLAPIIs

In a previous study, we constructed a bacterial expression, pQE-LAPII, for the heterologous production of BsLAPII in *E. coli* [26]. The mRNA of this construct encodes ten additional amino acids (MRGSHHHHHH) at the N-terminus of BsLAPII, which facilitates one-step purification of the enzyme with Ni^{2+}-NTA resin. In order to construct the poly-lysine-tagged BsLAPIIs, the DNA fragments amplified with LAPIIf/LAPIIr-Lys_3 and LAPIIf/LAPIIr-Lys_9 were restricted with *Bam*HI and *Hin*dIII, and inserted into the respective sites of pQE-30 to obtain pQE-LAPII-Lys_3 and pQE-LAPII-Lys_9, respectively. Analysis of the crude extracts from IPTG-induced *E. coli* M15 harboring either pQE-LAPII-Lys_3 or pQE-LAPII-Lys_9 revealed a predominant protein with apparent M_r of approximately 45 kDa (Fig. 1A), which compared well with the calculated mass of the poly-lysine-tagged translational product of the fusion gene. As a control, a 45-kDa protein band was also present in *E. coli* M15 (pQE-LAPII). Wild-type and poly-lysine-tagged BsLAPIIs in the crude extracts were further purified to nearly homogeneity by a Ni^{2+}-NTA agarose column (Fig. 1B). From 100 ml of bacterial culture corresponding to approximately 0.3 g of *E. coli* cells, the purification procedure resulted in a yield of 1.2–1.7 mg of the recombinant enzymes. The specific activity for BsLAPII, BsLAPII-Lys_3, and BsLAPII-Lys_9 was 45.6 ± 3.8, 42.3 ± 2.1, and 48.1 ± 3.9 U/mg protein, respectively.

3.2. Characterization of AuNP-COOH

For the reproducible immobilization of enzymes with an adequate orientation, highly stable gold nanoparticles were prepared by surface modification of citrate-reduced gold nanoparticles with MHA [33]. The AuNP reduced by citrate is known to be sufficiently hydrophilic but has a tendency to aggregate, depending on the micro-environment. This vulnerability was substantially improved to protect AuNP with a long aliphatic thiol with a carboxyl end group. The adsorption of MHA on gold nanoparticle surfaces was characterized by FT-IR spectroscopy. The AuNP-COOH spread on the ATR element showed C=O stretching band at 1710 cm^{-1} in its monomer state (Fig. 2). The peak frequencies 2918 and 2849 cm^{-1}, assigned as CH_2 asymmetric and symmetric bands, designates all-*trans* alkyl chains with minimal gauche conformation [34]. Water dispersible and highly stable characteristics of the present AuNPs might be attributed to the well close-packed alkyl chains serving as a physical barrier against

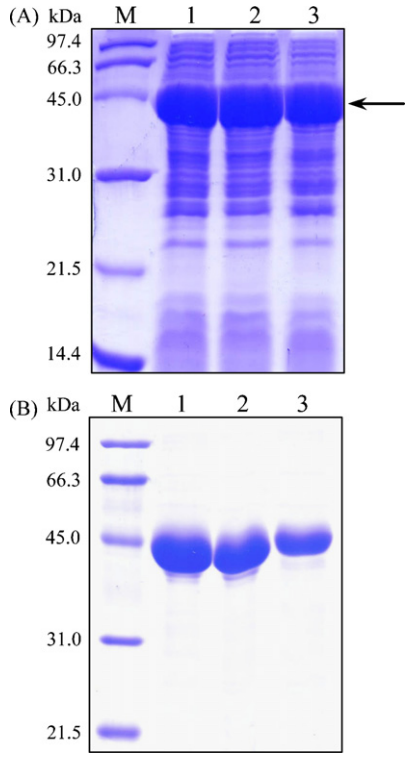

Fig. 1. SDS/PAGE analyses. (A) The crude extracts from *E. coli* M15 transformants were analyzed by 12% polyacrylamide–SDS gels and visualized by Coomassie brilliant staining. Lanes: M, protein size markers; 1, *E. coli* M15 (pQE-LAPII); 2, *E. coli* M15 (pQE-LAPII-Lys_3); 3, *E. coli* M15 (pQE-LAPII-Lys_9). (B) The purified wild-type and recombinant enzymes. Lanes: M, protein size markers; 1, BsLAPII; 2, BsLAPII-Lys_3; 3, BsLAPII-Lys_9.

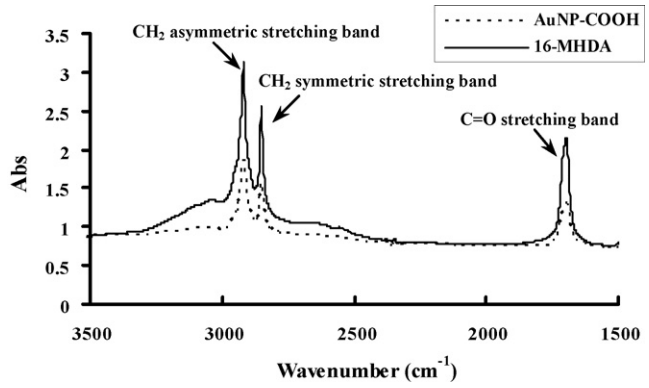

Fig. 2. FT-IR spectra of free MHA and MHA modified gold nanoparticles.

the formation of particle agglomerates. Fig. 3 shows a TEM image of highly monodisperse AuNPs spread on a copper grid with a dominant diameter of 16–20 nm. The high stability of the AuNP was manifested by the following two facts. First, AuNP solution in a vial was dried by continuous blowing of N_2 gas and was re-dispersed with distilled water. Second, the carboxylated AuNPs were washed out by centrifugation/re-dispersion cycles twice, and a working solvent was easily exchanged into methanol, DMSO, and Tris–HCl buffer. The control of surface properties of gold nanoparticle is extended one step further by the introduction of the concept of electrostatically driven layer [35]. The versatility of this approach resides in the nature of the interactions involved: the electrostatic attraction between oppositely charged molecules is nonspecific and has the least steric demand for all chemical bonds. The only requirement is the existence of multiple electrostatic binding points between the molecule and the target protein [35]. Based on this approach, the strategy of functionalizing a surface through electrostatic assembly has long been used for the purpose of biomolecule immobilizations [36–40]. Similarly, the electrostatic adsorption of ploy-lysine tag is employed as a facile way to immobilize BsLAPII onto the surface of gold nanoparticles.

The carboxylated AuNP functioned as a nano-supporter to immobilize recombinant enzyme with affinity Lys tags. It is noteworthy that the Lys-tagged BsLAPII tended to adsorb onto AuNP-COOH and no agglomerate was formed during the adsorption of the recombinant enzymes onto the carboxylated nanoparticles. The high stability could be attributed to negatively charged AuNP-COOH and relatively low p*I* value of the concerned protein (for BsLAPII, p*I* 5.04). One important merit of

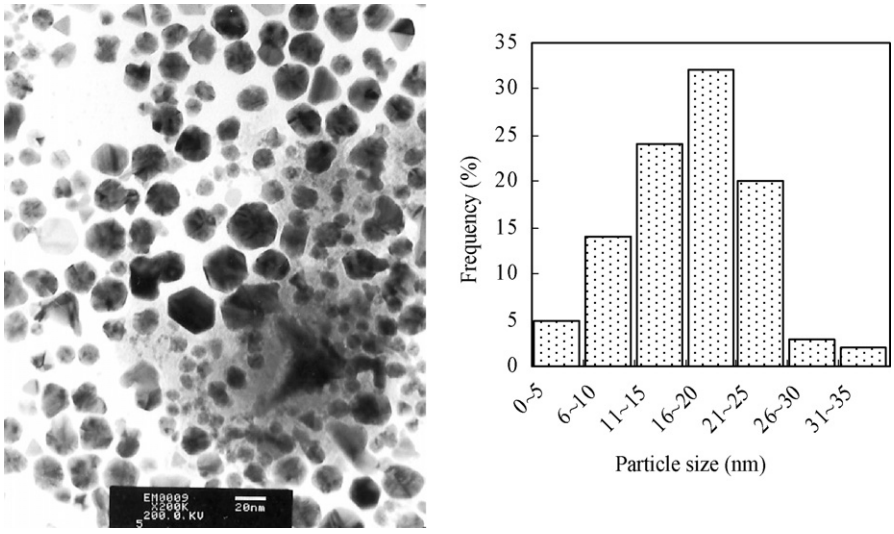

Fig. 3. A TEM image of citrate-reduced gold nanoparticles spread on a copper grid and size distribution of particles observed in the picture.

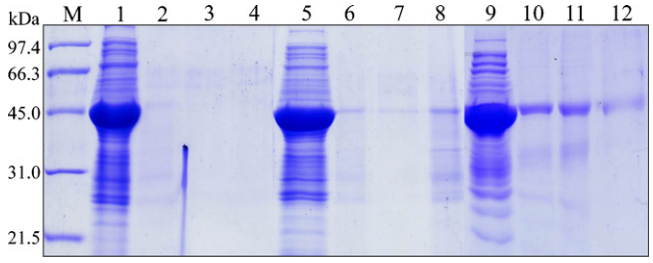

Fig. 4. Amounts of BsLAPII (lanes 2 and 3), BsLAPII-Lys$_3$ (lanes 6 and 7), and BsLAPII-Lys$_9$ (lanes 10 and 11) tethered on AuNP-COOH before and after the elution with 1 M NaCl solution, in comparison with the bands obtained by loading the tagged BsLAPII in the crude extract state (lane 1, BsLAPII; lane 5, BsLAPII-Lys$_3$; lane 9, BsLAPII-Lys$_9$). Lanes 4, 8 and 12 are the respective pellets of BsLAPII, BsLAPII-Lys$_3$ and BsLAPII-Lys$_9$ after the elution with 1 M NaCl.

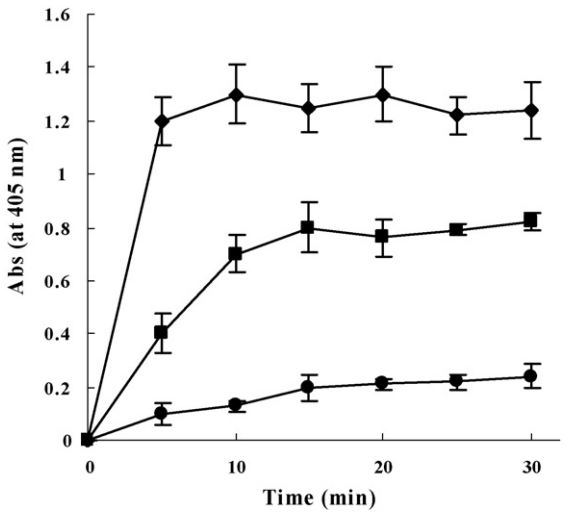

Fig. 5. Enzymatic activity assay of BsLAPII, BsLAPII-Lys$_3$, and BsLAPII-Lys$_9$ tethered on AuNP-COOH.

protein immobilization onto AuNP might be the controlled surface roughness, which assures relatively homogenous activities of adsorbed enzymes, compared to conventional polycrystalline gold surfaces.

3.3. Enzyme immobilization

The amounts of Lys-tagged BsLAPII immobilized on AuNP-COOH were analyzed by SDS/PAGE. In this experiment, Lys$_{3/9}$-tagged BsLAPII adsorbed onto AuNP-COOH was soaked with 1 M NaCl for 10 min, centrifuged, and the resulting pellet was analyzed by SDS/PAGE. As shown in Fig. 4, the amount of BsLAPII-Lys$_9$ remaining on the AuNP-COOH surface substantially reduced after elution with 1 M NaCl (lane 12). A less adsorption onto the nanoparticles was observed for BsLAP-Lys$_3$ (lane 6), while BsLAPII was hardly adsorbed AuNP-COOH. All these observations are consistent with the importance of positive charges of the tag in the large adsorption onto AuNP-COOH and the maintenance of enzyme activity [41,42]. Furthermore, BsLAPII-Lys$_3$ and BsLAPII-Lys$_9$ seems to be dominant absorbants for AuNP-COOH in the presence of other proteins (Fig. 4). A number of protein bands together with BsLAPII-Lys$_{3/9}$ existed in the stock solution, but the intensities of these protein bands were substantially reduced or even disappeared after the adsorption to AuNP-COOH. This relative specificity seems to be caused by faster adsorption of poly-lysine tag onto the nanoparticles than other non-tagged proteins.

The enzymatic activities of the BsLAPIIs on the surface of AuNP-COOH were investigated by monitoring the absorption characteristics of the substrate, Leu-*p*-NA, which develops a new band at 405 nm as it dissociates. As shown in Fig. 5, a series of measurements indicated that the enzymatic reaction in the AuNP-COOH solution (18 nM, 1 ml) containing BsLAPII-Lys$_9$ reached a saturation level within 5 min. Although the absorbance measurements of BsLAPII and BsLAPII-Lys$_3$ were performed at the same concentration of AuNP-COOH, substantially lower LAP activities were observed (Fig. 5). Taking the total amount of the immobilized BsLAPII-Lys$_9$ into account, 64% of the enzyme on an average was found to maintain its activity (Table 1). On the other hand, BsLAPII on AuNP-COOH demonstrated extremely low enzymatic activity of less than 0.1 μg/ml. Although the reduced activity of the immobilized (∼64%) seems to be caused by a surface-induced conformation change, diffusional limitation in this bound enzyme system might also affect the apparent activity without actually fouling the structure of individual protein. To address this issue, a kinetic experiment was performed to measure the initial rates of several Leu-*p*-NA concentrations with fixed amounts of free and immobilized BsLAPIIB-Lys$_9$. The results showed that both free and bound enzyme had a similar K_m value (0.97 mM *versus* 1.21 mM), implying that BsLAPIIB-Lys$_9$ on the surface of AuNP-COOH can be concluded not to be restricted by the substrate diffusion at the working concentration (∼2.0 mM). Based on these observations, it is obvious that BsLAPII-Lys$_9$ was efficiently adsorbed onto AuNP-COOH through electrostatic attraction with its activity maintained, while most BsLAPII was nonspecifically adsorbed with a trace activity. However, it should be noted that a substantial amount of BsLAPII-Lys$_9$ was still nonspecifically adsorbed, and that only 64% of the adsorbed enzyme demonstrated the LAP activity. The reduced activity appears to be caused by hydrophobic interactions between the protein and the underlying hydrophobic region beneath the carboxyl group [43].

3.4. pH and temperature stability of free and immobilized BsLAPII-Lys$_9$

Fig. 6A shows plots of the catalytic activity of free BsLAPII-Lys$_9$ molecules in solution and BsLAPII-Lys$_9$ bound to the nanogold template for reactions carried out after preincubating the enzyme/bioconjugate as a function of solution pH in the range 2–9. It is seen that the optimum activity in both the cases is at pH 8, with a marginal loss in catalytic activity at pH 7. At pH 4, however, free BsLAPII-Lys$_9$ molecules retained only 42% of the activity recorded at pH 8, while the immobilized enzyme retained as much as 53% of the catalytic activity recorded at pH 8. Even at pH 3, BsLAPII-Lys$_9$ in the bioconjugate material showed significant catalytic activity.

Table 1
Total amounts of recombinant BsLAPIIs with distinct affinity tags and amounts

Affinity tag in the enzyme	Amount of immobilized enzyme (SDS/PAGE) (μg/ml)	Elution by 1 M NaCl[a] (μg/ml)		Amount of active enzyme (UV/vis) (μg/ml)	Surviving activity (%)
		Eluted (Bradford)	Remaining (SDS/PAGE)		
His_6/Lys_9	9.7	5.3	2.2	6.2	64
His_6/Lys_3	2.5	0.9	1.3	1.0	40
His_6	0.2	<0.1	<0.1	<0.1	–[b]

[a] The Bradford method quantified all the proteins eluted by 1 M NaCl, while SDS/PAGE results estimated a specific band after the gel-electrophoresis.
[b] –, not determined.

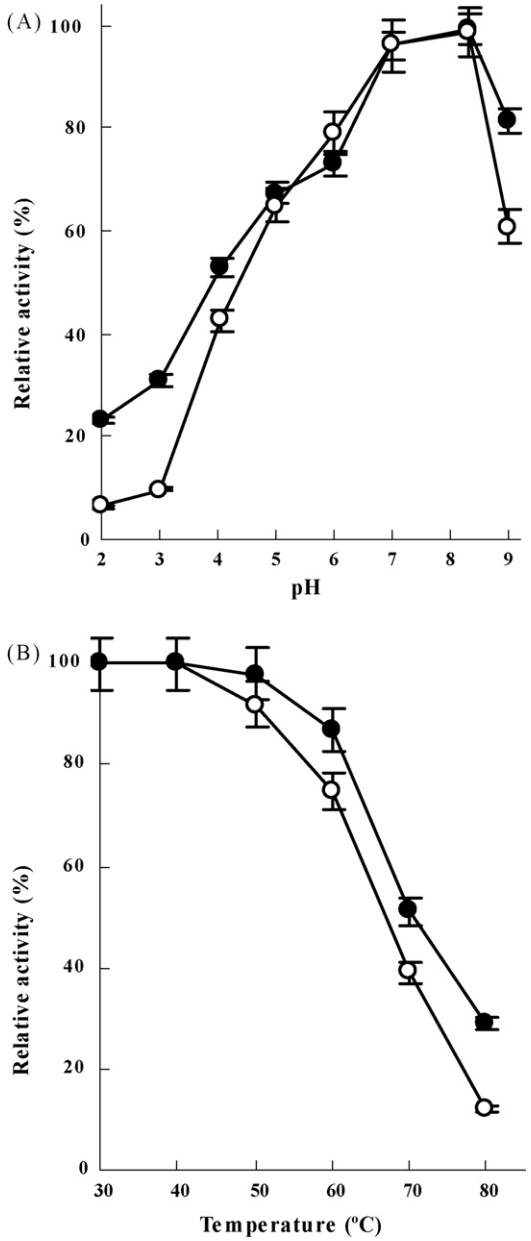

Fig. 6. Effects of pH and temperature on free and bioconjugate enzyme. (A) pH-dependent catalytic activity of free BsLAPII-Lys_9 in solution (open circles) and BsLAPII-Lys_9 in the nanogold template (solid circles). The 100% relative activity for BsLAPII-Lys_9 and AuNP-COOH::BsLAPII-Lys_9 corresponded to 36.7 and 32.1 U/ml, respectively. (B) Temperature-dependent catalytic activity of free BsLAPII-Lys_9 in solution (open circles) and BsLAPII-Lys_9 in the nanogold template (solid circles). The 100% relative activity for BsLAPII-Lys_9 and AuNP-COOH::BsLAPII-Lys_9 corresponded to 41.7 and 39.2 U/ml, respectively.

Fig. 6B shows plots of the variation in catalytic activity of free BsLAPII-Lys_9 molecules in solution and BsLAPII-Lys_9 bound to the nanogold template as a function of temperature stability. At higher temperatures, dramatic differences were observed in catalytic activity of the enzyme in the two cases. The free enzyme retained 37% of the original catalytic activity at 70 °C, while the BsLAPII-Lys_9-nanogold bioconjugate retained 52% of the relative activity at the same temperature. Such enhancement in stability of immobilized enzymes as a function of temperature has been observed for pepsin bound to alumina nanoparticles [44], and for other enzymes immobilized on different supports [45–47].

3.5. Reusability

The immobilized BsLAPII-Lys_3 and BsLAPII-Lys_9 were repeatedly used to hydrolyze Leu-*p*-NA in batch reactions. BsLAPII-Lys_3- and BsLAPII-Lys_9-nanogold materials (∼0.21 mg for both samples) in 2 ml of 50 mM Tris–HCl buffer (pH 8.0) containing 2 mM Leu-*p*-NA, 1 mM $CoCl_2$ were shaken (50 rpm) at 60 °C for 10 min each time. The enzyme-nanogold bioconjugate materials were then centrifuged at 12,000 × *g* for 5 min, washed once with 2 ml of 50 mM Tris–HCl buffer (pH 8.0), and reused for another run. LAP activity in the supernatants was determined under the standard assay conditions. Table 2 lists the catalytic activity calculated from reaction of the BsLAPII-Lys_3- and BsLAPII-Lys_9-nanogold bioconjugate materials over five sequential reuse cycles. The catalytic activity of the BsLAPII-Lys_3-nanogold material fell rapidly, completely losing activity by the fourth run of reaction. On the other hand, BsLAPII-Lys_9-nanogold material showed ∼75% of catalytic

Table 2
Relative activity of BsLAPII-Lys_3- and BsLAPII-Lys_9-nanogold bioconjugate materials during successive reuses

No. of cycles	Relative activity (%)[a]	
	AuNP-COOH::BsLAPII-Lys_3	AuNP-COOH::BsLAPII-Lys_9
1	100	100
2	37	75
3	15	61
4	2	39
5	0	24

[a] LAP activity assayed in the first cycle of reaction was taken as 100%, which corresponds to 27.2 and 30.9 U/ml for AuNP-COOH::BsLAPII-Lys_3 and AuNP-COOH::BsLAPII-Lys_9, respectively. The experiments were performed in triplicate and data were expressed as mean values.

activity after the first reuse cycle and retained 24% of the initial catalytic activity at the fifth run of reaction. These results clearly underline the remarkable reuse characteristic of the BsLAPII-Lys_9-nanogold bioconjugate material.

4. Conclusion

In summary, poly-lysine-tagged BsLAPII can be successfully immobilized on the surface of carboxyl-terminated alkanethiol modified AuNPs. The substrates are easily accessible to the immobilized enzyme, thus mimicking the free enzyme in solution for all practical purposes. As compared with free BsLAPII, the lysine-tagged enzyme in the bioconjugate system shows enhanced stability toward more harsh temperature condition. Moreover, the enzyme-nanogold bioconjugate material exhibits excellent reuse characteristic. Based on these advantages, the BsLAPII/AuNP-COOH bioconjugates can be expected as catalytic nanodevice to construct nanoreactors based on LAP reaction for biological applications.

Acknowledgements

We are grateful for the financial support from the National Science Council of Taiwan (NSC 95-2313-B-415-001 and NSC 95-2313-B-415-012-MY3). Helpful discussion and manuscript revision provided by Professor Wen-Hwei Hsu, Institute of Molecular Biology, National Chung Hsing University are also acknowledged.

References

[1] S.G. Penn, L. He, M.J. Natan, Curr. Opin. Chem. Biol. 7 (2003) 609–616.
[2] Y. Xiao, F. Patolsky, E. Katz, J.F. Hainfeld, I. Willner, Science 299 (2003) 1877–1881.
[3] E. Katz, I. Willner, Angew. Chem. Int. Ed. 43 (2004) 6042–6108.
[4] B. Willner, E. Katz, I. Willner, Curr. Opin. Biotechnol. 17 (2006) 589–596.
[5] I. Willner, B. Willner, E. Katz, Bioelectrochemistry 70 (2007) 2–11.
[6] M.C. Daniel, D. Astruc, Chem. Rev. 104 (2004) 293–346.
[7] E.V. Shevchenko, D.V. Talapin, N.A. Kotov, S. O'Brien, C.B. Murray, Nature 439 (2006) 55–59.
[8] P.R. Selvakannan, S. Mandal, S. Phadtare, R. Pasricha, M. Sastry, Langmuir 19 (2003) 3545–3549.
[9] P.R. Selvakannan, S. Mandal, S. Phadtare, A. Gole, R. Pasricha, S. Adyanthava, M. Sastry, J. Colloid Interface Sci. 269 (2004) 97–102.
[10] F. Patolsky, M. Zayas, E. Katz, I. Willner, Anal. Chem. 71 (1999) 3171–3180.
[11] C.M. Niemeyer, B. Ceyhan, Angew. Chem. Int. Ed. 40 (2001) 3685–3688.
[12] A. Cole, C. Dash, V. Ramakrishnan, S.R. Sainkar, A.B. Mandle, M. Rao, M. Sastry, Langmuir 17 (2001) 1674–1679.
[13] A. Cole, C. Dash, C. Soman, S.R. Sainkar, M. Rao, M. Sastry, Bioconjugate Chem. 12 (2001) 684–690.
[14] T.H. Ha, J.Y. Jeong, B.H. Chung, Chem. Commun. (2005) 3959–3961.
[15] A.G. Kanaras, Z. Wang, A.D. Bates, R. Cosstick, M. Brust, Angew. Chem. Int. Ed. 42 (2003) 191–194.
[16] W.J. Qin, L.Y. Yung, Langmuir 21 (2005) 11330–11334.
[17] A.L. Crumbliss, J.G. Stonehuerner, R.W. Henkens, J. Zhao, J.P. O'Daly, Biosens. Bioelectron. 8 (1993) 331–337.
[18] N.O. Fischer, C.M. Mclntosh, J.M. Simard, V.M. Rotello, Proc. Natl. Acad. Sci. U.S.A. 99 (2002) 5018–5023.
[19] J.M. Abad, S.F.L. Mertens, M. Pita, V.M. Fernández, D.J. Schiffrin, J. Am. Chem. Soc. 127 (2005) 5689–5694.
[20] M. Zheng, X. Huang, J. Am. Chem. Soc. 126 (2004) 12047–12054.
[21] M. Zheng, Z. Li, X. Huang, Langmuir 11 (2004) 4226–4235.
[22] A. Taylor, FASEB J. 7 (1993) 290–298.
[23] A. Taylor, Trends Biochem. Sci. 18 (1993) 167–171.
[24] R.J. Fitzgerald, G. O'Cuinn, Biotechnol. Adv. 24 (2006) 234–237.
[25] M.J. Wyvratt, Clin. Physiol. Biochem. 6 (1988) 217–229.
[26] L.Y. Kuo, G.Y. Hwang, Y.J. Lai, S.L. Yang, L.L. Lin, Curr. Microbiol. 47 (2003) 40–45.
[27] L.Y. Kuo, G.Y. Hwang, S.L. Yang, Y.W. Hua, W. Chen, L.L. Lin, Protein J. 23 (2004) 295–302.
[28] G.Y. Hwang, L.Y. Kuo, M.R. Tsai, S.L. Yang, L.L. Lin, Antonie van Leewenhoek 87 (2005) 355–359.
[29] U.K. Laemmli, Nature 227 (1970) 680–685.
[30] M.M. Bradford, Anal. Biochem. 72 (1976) 248–254.
[31] J.M. Prescott, S.H. Wilkes, Methods Enzymol. 45 (1976) 530–543.
[32] P.C. Lee, D. Meisel, J. Phys. Chem. 86 (1982) 3391–3395.
[33] K. Aslan, V.H. Perez-Luna, Langmuir 18 (2002) 6059–6065.
[34] A. Gericke, H. Hühnerfuss, Thin Solid Films 245 (1994) 74–85.
[35] G. Decher, Science 277 (1997) 1232–1237.
[36] C.E. Jordan, B.L. Frey, S. Kornguth, R.M. Corn, Langmuir 10 (1994) 3642–3648.
[37] B.L. Frey, R.M. Corn, Anal. Chem. 68 (1996) 3187–3193.
[38] C.E. Jordan, A.G. Frutos, A.J. Thiel, R.M. Corn, Anal. Chem. 69 (1997) 4939–4947.
[39] A.J. Thiel, A.G. Frutos, C.E. Jordan, R.M. Corn, L.M. Smith, Anal. Chem. 69 (1997) 4948–4956.
[40] S.D. Gillmor, A.J. Thiel, T.C. Strother, L.M. Smith, M.G. Lagally, Langmuir 16 (2000) 7223–7228.
[41] K. Terpe, Appl. Microbiol. Biotechnol. 60 (2003) 523–533.
[42] S.V.P. Barreira, F. Silva, Langmuir 19 (2004) 10324–10331.
[43] R. Hong, N.O. Fischer, A. Verma, C.M. Goodman, T. Emrick, V.M. Rotello, J. Am. Chem. Soc. 126 (2004) 739–743.
[44] J. Li, J. Wang, V.G. Gavalas, D.A. Atwood, L.G. Bachas, Nano Lett. 3 (2003) 55–58.
[45] H. Takahashi, B. Li, T. Sasaki, C. Miyazaki, T. Kajino, S. Inagaki, Chem. Mater. 12 (2000) 3301–3305.
[46] S. Akgol, Y. Yalcinkaya, G. Bayramoglu, A. Denizli, M.Y. Arica, Process Biochem. 38 (2002) 675–683.
[47] S. Phadtare, V.P. Vinod, P.P. Wadgaonkar, M. Rao, M. Saatry, Langmuir 20 (2004) 3717–3723.